frontiers | Frontiers in Genetics

TYPE Original Research
PUBLISHED 12 December 2022
DOI 10.3389/fgene.2022.992995

OPEN ACCESS

EDITED BY
Prakashbabu Phanithi,
University of Hyderabad, India

REVIEWED BY
Zheng He,
Qilu Hospital of Shandong University, China
Emil Bulatov,
Kazan Federal University, Russia

*CORRESPONDENCE
MeiHua Li,
limeihua2000@sina.com
YeYu Zhao,
zyp19850922@126.com

†These authors have contributed equally to this work

SPECIALTY SECTION
This article was submitted to Cancer Genetics and Oncogenomics, a section of the journal Frontiers in Genetics

RECEIVED 13 July 2022
ACCEPTED 02 December 2022
PUBLISHED 12 December 2022

CITATION
Zhu H, Wan Q, Tan J, Ouyang H, Pan X, Li M and Zhao Y (2022), A novel prognostic signature of cuproptosis-related genes and the prognostic value of FDX1 in gliomas.
Front. Genet. 13:992995.
doi: 10.3389/fgene.2022.992995

A novel prognostic signature of cuproptosis-related genes and the prognostic value of FDX1 in gliomas

HuaXin Zhu[1,2†], Qinsi Wan[3†], Jiacong Tan[1,2], Hengyang Ouyang[4], Xinyi Pan[4], MeiHua Li[1*] and YeYu Zhao[1*]

[1]Department of Neurosurgery, The First Affiliated Hospital of Nanchang University, Nanchang, Jiangxi, China, [2]Medical Innovation Center, The First Affiliated Hospital of Nanchang University, Nanchang, Jiangxi, China, [3]Department of Gastroenterology, The First Affiliated Hospital of Nanchang University, Nanchang, Jiangxi, China, [4]Huankui Academy, Nanchang University, Nanchang, Jiangxi, China

Background: Gliomas are the most common malignant tumors of the central nervous system, with extremely bad prognoses. Cuproptosis is a novel form of regulated cell death. The impact of cuproptosis-related genes on glioma development has not been reported.

Methods: The TCGA, GTEx, and CGGA databases were used to retrieve transcriptomic expression data. We employed Cox's regressions to determine the associations between clinical factors and cuproptosis-related gene expression. Overall survival (OS), disease-specific survival (DSS), and progression-free interval (PFI) were evaluated using the Kaplan-Meier method. We also used the least absolute shrinkage and selection operator (LASSO) regression technique.

Results: The expression levels of all 10 CRGs varied considerably between glioma tumors and healthy tissues. In glioma patients, the levels of CDKN2A, FDX1, DLD, DLAT, LIAS, LIPT1, and PDHA1 were significantly associated with the OS, disease-specific survival, and progression-free interval. We used LASSO Cox's regression to create a prognostic model; the risk score was (0.882340) *FDX1 expression + (0.141089) *DLD expression + (−0.333875) *LIAS expression + (0.356469) *LIPT1 expression + (−0.123851) *PDHA1 expression. A high-risk score/signature was associated with poor OS (hazard ratio = 3.50, 95% confidence interval 2, −4.55, log-rank $p < 0.001$). Cox's regression revealed that the FDX1 level independently predicted prognosis; FDX1 may control immune cell infiltration of the tumor microenvironment.

Conclusion: The CRG signature may be prognostic in glioma patients, and the FDX1 level may independently predict glioma prognosis. These data may afford new insights into treatment.

KEYWORDS

gliomas, cuproptosis, FDX1, prognosis, prognostic signature

1 Introduction

Malignant tumors of the central nervous system (CNS) have one of the poorest prognoses of all cancers; life is shortened by about 20 years (Rouse et al., 2010; Reifenberger et al., 2017). More than 70% of all malignant CNS tumors are gliomas; such tumors are the most common CNS tumors (Gilbert et al., 2014). Half of all newly diagnosed gliomas are very malignant glioblastomas; the median patient survival is approximately 12 months (Gramatzki et al., 2016; Quinones and Le, 2018). Over the last decade, isocitrate dehydrogenase (IDH) mutations, chromosome 1p/19q deletions, MGMT and TERT promoter methylations, and histone mutations have all served as glioma biomarkers; these markers play key roles in glioma classification and treatment decisions (Chen et al., 2017; Brito et al., 2019). Despite great advances in surgery, radiotherapy, chemotherapy, and targeted therapy, almost all malignant gliomas recur, associated with poor prognoses. Better prognostic models are urgently required.

Although heavy metal ions are crucial micronutrients, ion levels that are too low or excessive may trigger controlled cell death (Wang et al., 2022a) *via* activation of various subprograms. For example, ferroptosis is an iron-dependent form of uncontrolled, lipid peroxidation-induced, oxidative cell death (Dixon et al., 2012; Liang et al., 2019). Recently, Tsvetkov et al. (2022) found that intracellular copper (Cu) triggered a unique form of controlled cell death termed "cuproptosis," which differed from apoptosis, necrosis, autophagy, and ferroptosis. The lipoylated acylated components of the tricarboxylic acid (TCA) cycle bind directly to copper, imparting protein stress and eventual cell death (Hatori et al., 2016). Recent studies have shown that cancer patients exhibit much higher serum and tumor tissue copper levels than healthy people (Blockhuys et al., 2017; Ge et al., 2022). Dysregulation of copper homeostasis may be cytotoxic; changes in intracellular copper levels may influence cancer development and spread (Ishida et al., 2013; Babak and Ahn, 2021). However, any relationship between cuproptosis and glioma progression remains unknown. This is our topic here; glioma cuproptosis-related gene (CRG) expression is of clinical and potential prognostic utility.

2 Methods

2.1 Data acquisition

The glioma RNA-seq data of TCGA and the corresponding normal tissue data of GTEx derived *via* uniform toil processing were downloaded from UCSCXENA (https://xenabrowser.net/datapages/). The Human Protein Atlas database (https://www.proteinatlas.org/) was used to examine protein expression in normal and glioma tissues. We also downloaded RNA-seq data and clinical information (DataSet ID: mRNAseq_693) of glioma samples from the CGGA database (http://www.cgga.org.cn/); we used this information to externally validate the survival analyses.

2.2 Differential expression analysis

We integrated the TCGA and GTEx databases and then sought differences in CRG expression levels between glioma and normal tissue samples. We drew receiver operating characteristic (ROC) curves to assess the predictive accuracies of CRG levels. The relationships between CRG levels and clinicopathological features were explored using the TCGA database and validated employing the CGGA database. The R package DESeq2 (ver. 1.26.0) was used to distinguish the expression levels of mRNAs associated with low and high risks of progression; we identified differentially expressed genes (DEGs) using the thresholds of $\log_2$ (FC) > 2.0 and an adjusted p-value <0.05. The DEGs were displayed using volcano plots and heat maps.

2.3 Prognostic signatures of cuproptosis-related genes

Useful features were selected using the least absolute shrinkage and selection operator (LASSO) regression algorithm; 10-fold cross-validation followed and the R package glmnet was used to analyze the data. First, multifactorial Cox's regression was performed, followed by iteration using a step function. The optimal model was selected. We used the log-rank test and Cox's proportional hazards regression to derive p-values and hazard ratios with 95% confidence intervals (CIs); then we drew Kaplan-Meier curves. We used the decision curve analysis R package ggDCA to construct the prognostic signature of CRG levels.

2.4 Functional and pathway enrichment analyses

We employed the R clusterProfiler package to perform Gene Ontology (GO) and Kyoto Encyclopedia of Genes and Genomes (KEGG) enrichment analyses and displayed the findings using the R packages dplyr and ggplot2. We uploaded the DEGs to Metascape (an online tool for gene function/annotation analysis; https://metascape.org/).

2.5 Construction of a prognostic model and external validation

We sought prognostic factors among clinical variables, performed univariate and multivariate Cox's regressions, and

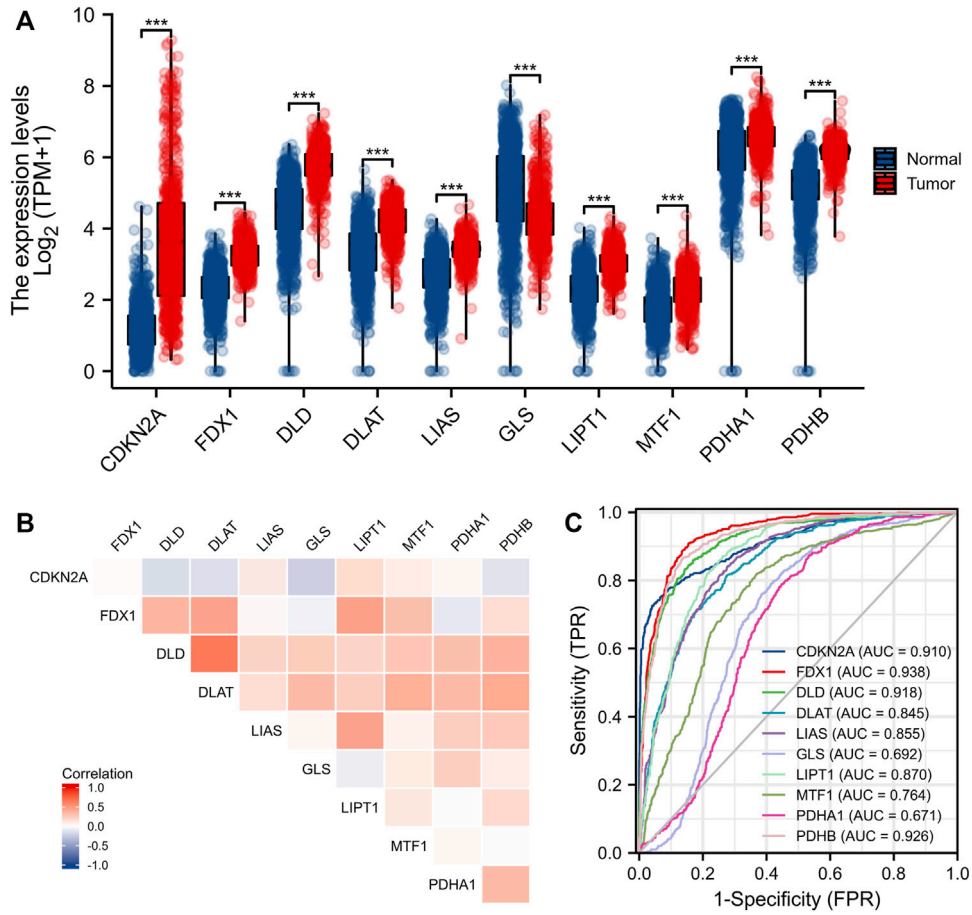

FIGURE 1
Expression of CRGs in gliomas. **(A)** Expression of 10 CRGs in gliomas and normal tissues. **(B)** Correlation between CRGs expression. **(C)** Diagnostic value of CRGs in gliomas. *$p < 0.05$, **$p < 0.01$, ***$p < 0.001$. CRGs: cuproptosis-related genes.

derived an optimal prognostic model. The R package rms was used to create a nomogram that predicted prognosis. Harrell concordance index (C-index) calibration plots were drawn to evaluate the reliabilities and accuracies of the prognostic models. Kaplan-Meier curves were drawn to compare the differences between paired groups in terms of overall survival (OS), disease-specific survival (DSS), and progression-free interval (PFI).

2.6 Evaluation of immune cell infiltration

The Tumor Immune Estimation Resource (Timer) method of the R package immunedeconv was used to seek correlations between immune cell activities, and the constructed models and the gene expression levels *per se*. The R package ggstatsplot was employed to derive correlations between gene expression levels and immune system scores; the R package pheatmap was used to identify multi-gene correlations. We used the single-sample Gene Set Enrichment Analysis (ssGSEA) technique of the R GSVA package to measure the levels of 24 immune cell types associated with glioma infiltration. The R package is based on the TCGA database. We used Spearman analyses to derive correlations between quantitative variables that were not normally distributed.

2.7 Statistical analysis

Paired samples were evaluated using the Wilcoxon signed-rank test; unpaired samples were assessed employing the Wilcoxon rank-sum test. We used the Kruskal–Wallis test, the Wilcoxon signed-rank test, and logistic regression to explore the relationships between clinical characteristics and CRG expression levels. Either the chi-square or the Fisher exact test was used to investigate relationships between CRG expression levels and the clinical characteristics. R software ver. 4.0.3 was employed for all statistical analyses (R Foundation for Statistical Computing, Vienna, Austria). A p-value <0.05 was considered significant.

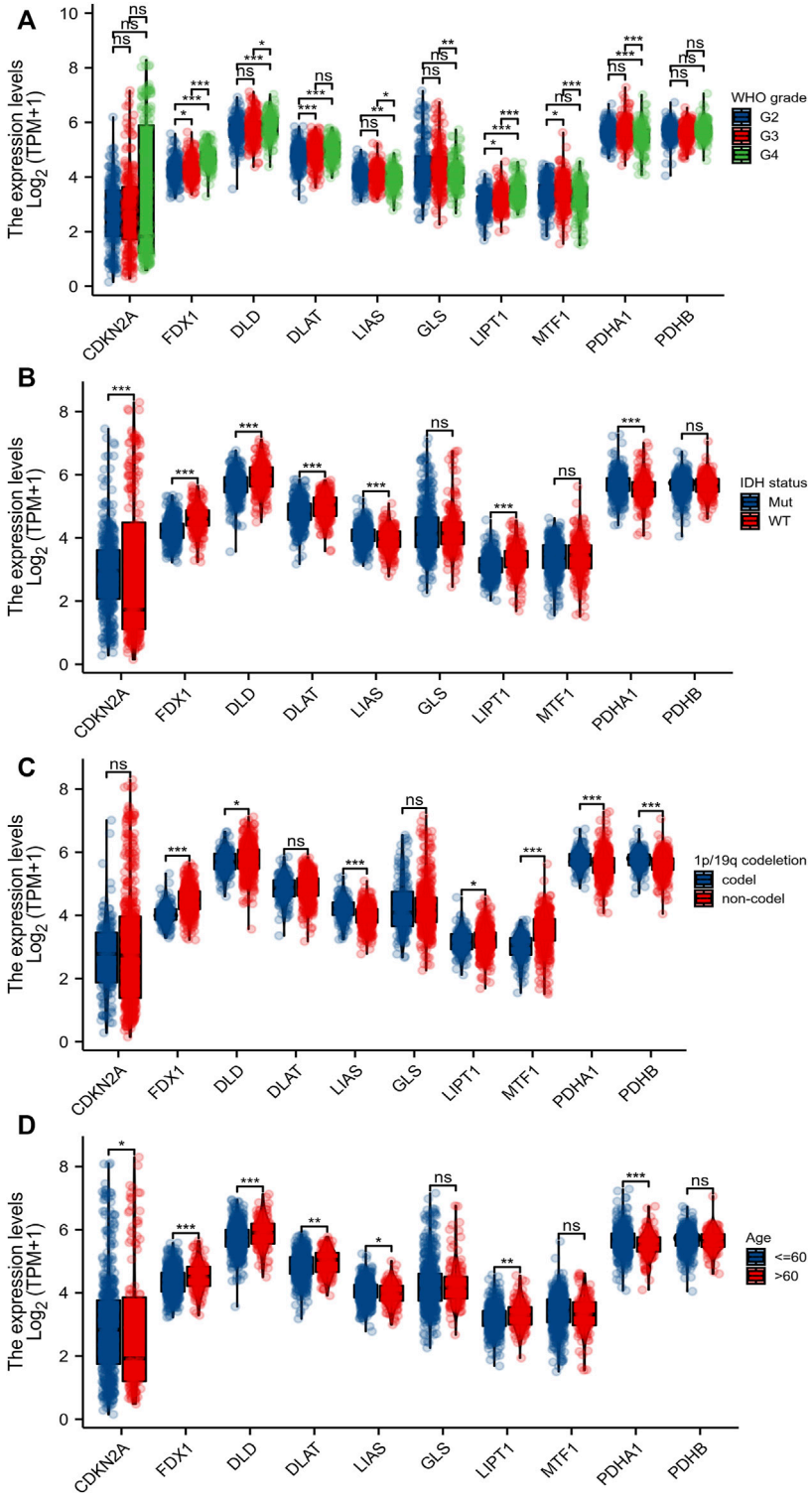

FIGURE 2
Relationship between CRGs and clinicopathological features. The association of 10 CRGs expression with WHO grade **(A)**, IDH status **(B)**, 1p/19q codeletion **(C)**, and age **(D)** in gliomas from TCGA database. *$p < 0.05$, **$p < 0.01$, ***$p < 0.001$. CRGs: cuproptosis-related genes.

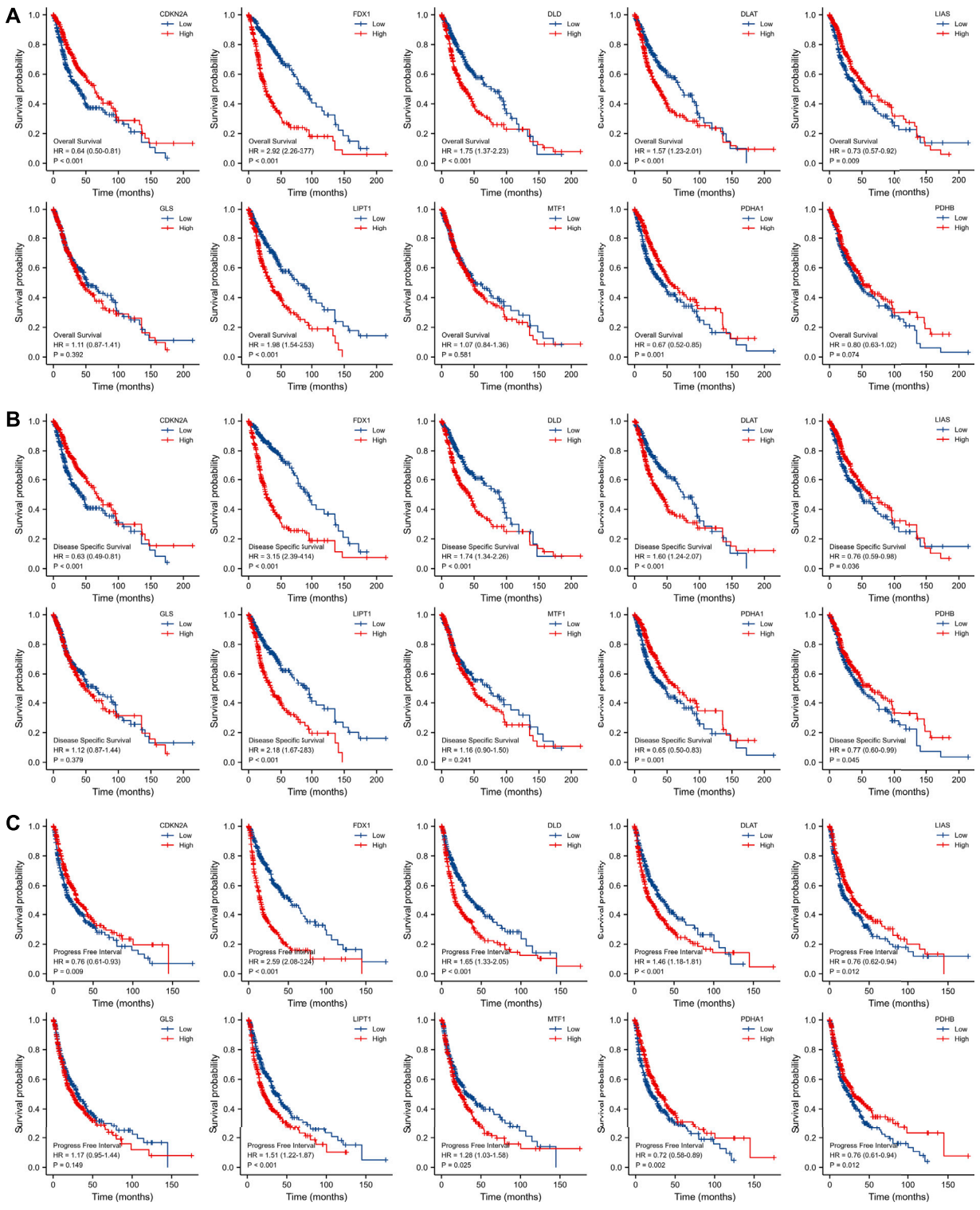

FIGURE 3
Survival analysis of OS **(A)**, DSS **(B)** and PFI **(C)** of 10 CRGs in gliomas patients from TCGA database. OS: overall survival, DSS: disease specific survival, PFI: progress free interval, CRGs: cuproptosis-related genes.

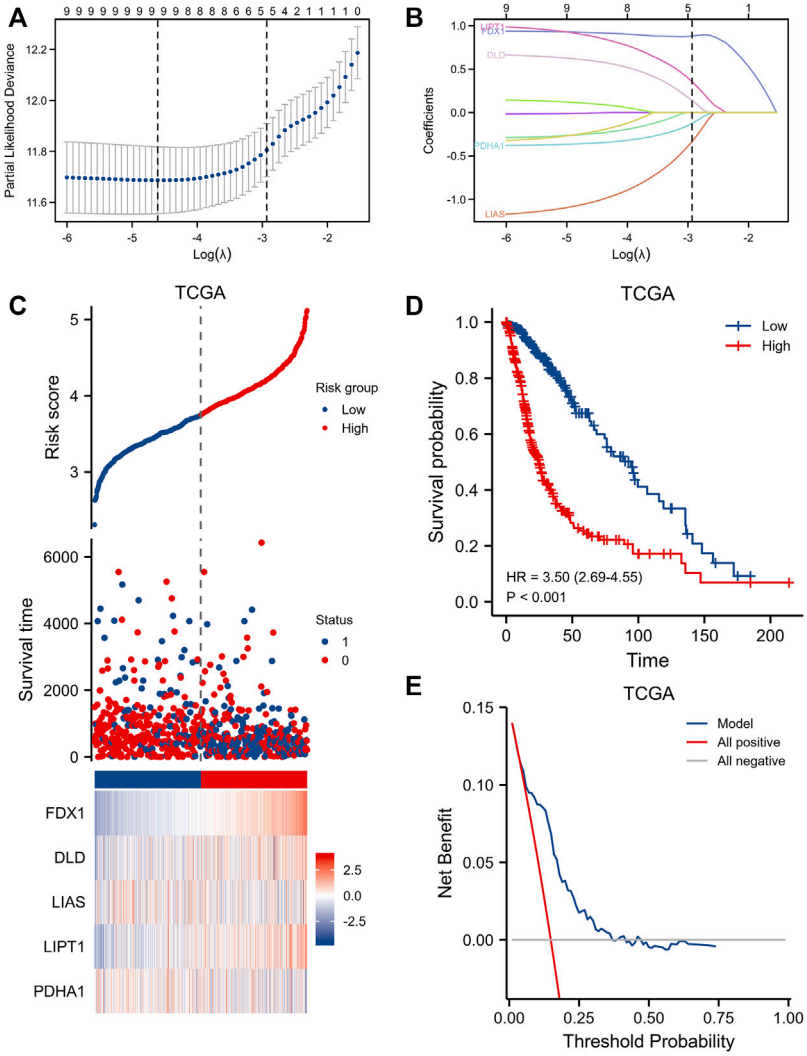

FIGURE 4
Clinical relevance of CRGs in the gliomas patients of TCGA. **(A,B)** LASSO regression analysis and partial likelihood deviance of the CRGs. **(C)** distribution of risk score, survival status and the expression of prognostic gliomas, **(D)** Kaplan–Meier plot of the CRGs signature and overall survival, **(E)** Decision curve analysis of CRGs signature for predicting survival status.

3 Results

3.1 CRG expression levels in glioma patients

Eleven genes (CDKN2A, DLD, DLAT, FDX1, GLS, LIAS, LIPT1, MTF1, PDHA1, and PDHB) are closely associated with cuproptosis. We found that only the expression level of GLS was significantly decreased in gliomas (compared to normal tissues); the levels of all other CRGs increased significantly (Figure 1A). We sought correlations between the levels of different CRGs (Figure 1B). We performed receiver operating characteristic curve (ROC) analyses to assess whether various CRG levels aided glioma detection; the areas under the curves (AUCs) were >0.9 for CDKN2A, FDX1, DLD, and PDHB (Figure 1C). Levels of FDX1, LIAS, LIPT1, DLD, DLAT, MTF1, and PDHA1 were associated with the World Health Organization (WHO) clinical grade (Figure 2A); levels of CDKN2A, DLAT, LIAS, LIPT1 FDX1, DLD, and PDHA1 with were associated with IDH status (Figure 2B); levels of FDX1, LIPT1, MTF1, PDHA1, DLD, LIAS, and PDHB were associated with 1p19q co-deletion (Figure 2C); and levels of CDKN2A, DLD, DLAT, LIAS, LIPT1, FDX1 and PDHA1 levels were associated with age (Figure 2D).

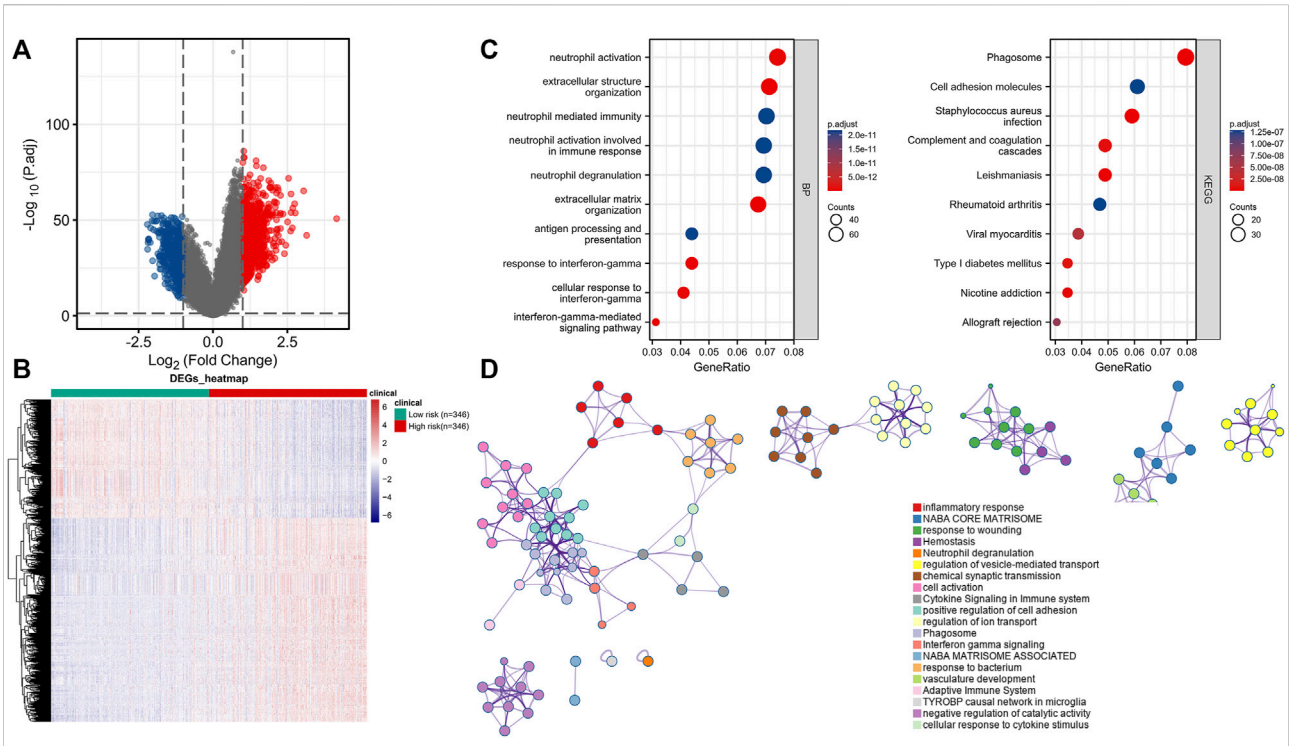

FIGURE 5
Functional enrichment analysis for CRGs signature in gliomas patients. **(A)** Volcano Plot of differentially expressed genes (DEGs) screened based on CRGs signature. **(B)** Gene set enrichment analysis of Gene Ontology biological process (GO-BP). **(C)** Gene set enrichment analysis of Kyoto Encyclopedia of Genes and Genomes (KEGG). **(D)** Network and bar chart of enrichment analysis results drawn by Metascape.

3.2 The survival analyses of CRGs in gliomas patients

Patients of the TCGA database expressing high levels of FDX1 (hazard ratio [HR] = 2.92 [95% confidence interval, CI] 2.26–3.77, log-rank $p < 0.001$); DLD (HR = 1.75 [1.37–2.23], log-rank $p < 0.001$); DLAT (HR = 1.57 [1.23–2.01], log-rank $p < 0.001$); and LIPT1 [HR = 1.98 (1.54–2.53), log-rank $p < 0.001$]; and low levels of CDKN2A [HR = 0.64 (0.50–0.81), log-rank $p < 0.001$]; LIAS [HR = 0.73 (0.57–0.92), log-rank $p = 0.009$]; and PDHA1 [HR = 0.67 (0.52–0.85), log-rank $p = 0.001$] experienced poorer OS than others (Figure 3A). Poor DSS was associated with high-level expression of FDX1 [HR = 3.15 (2.39–4.14), log-rank $p < 0.001$]; DLD [HR = 1.74 (1.34–2.26), log-rank $p < 0.001$]; DLAT [HR = 1.60 (1.24–2.07), log-rank $p < 0.001$]; and LIPT1 [HR = 2.18 (1.67–2.83), log-rank $p < 0.001$]; and low-level expression of CDKN2A [HR = 0.63 (0.49–0.81), log-rank $p < 0.001$]; LIAS [HR = 0.76 (0.59–0.98), log-rank $p = 0.036$]; PDHA1 [HR = 0.65 (0.50–0.83), log-rank $p = 0.001$]; and PDHB [HR = 0.77 (0.60–0.99), log-rank $p = 0.045$] (Figure 3B). PFI was affected by the levels of CDKN2A [HR = 0.76 (0.61–0.93), log-rank $p = 0.009$]; FDX1 [HR = 2.59 (2.08–3.24), log-rank $p < 0.001$]; DLD [HR = 1.65 (1.33–2.05), log-rank $p < 0.001$]; DLAT [HR = 1.46 (1.18–1.81), log-rank $p < 0.001$]; LIAS [HR = 0.76 (0.62–0.94), log-rank $p = 0.012$]; LIPT1 [HR = 0.51 (1.22–1.87), log-rank $p < 0.001$]; MTF1 [HR = 1.28 (1.03–1.58), log-rank $p < 0.001$]; PDHA1 [HR = 0.72 (0.58–0.89), log-rank $p = 0.002$]; and PDHB [HR = 0.76 (0.61–0.94), log-rank $p = 0.012$] (Figure 3C).

3.3 Construction of a CRG-derived prognostic gene signature

LASSO Cox's regression generated a five-gene signature (Figures 4A, B): Risk Score = (0.882340) *FDX1 expression + (0.141089) *DLD expression + (−0.333875) *LIAS expression + (0.356469) *LIPT1 expression + (−0.123851) *PDHA1 expression. We found a significant correlation between a high risk score and poor OS [HR = 3.50 (2.69–4.55), log-rank $p < 0.001$] (Figures 4C,D). Decision curve analysis in terms of OS prediction showed that the signature performed well [C-index 0.758 (0.743–0.772)] (Figure 4E). The CGGA database was utilized for external validation; we retrieved all data on glioma patients. As for TCGA patients, CGGA individuals with higher risk scores evidenced significantly shorter OS [HR = 1.68 (1.38–2.05), log-rank $p < 0.001$] (Supplementary Figure S1). The clinical information of TCGA and CGGA datasets were provided in Supplementary Tables S1, S2.

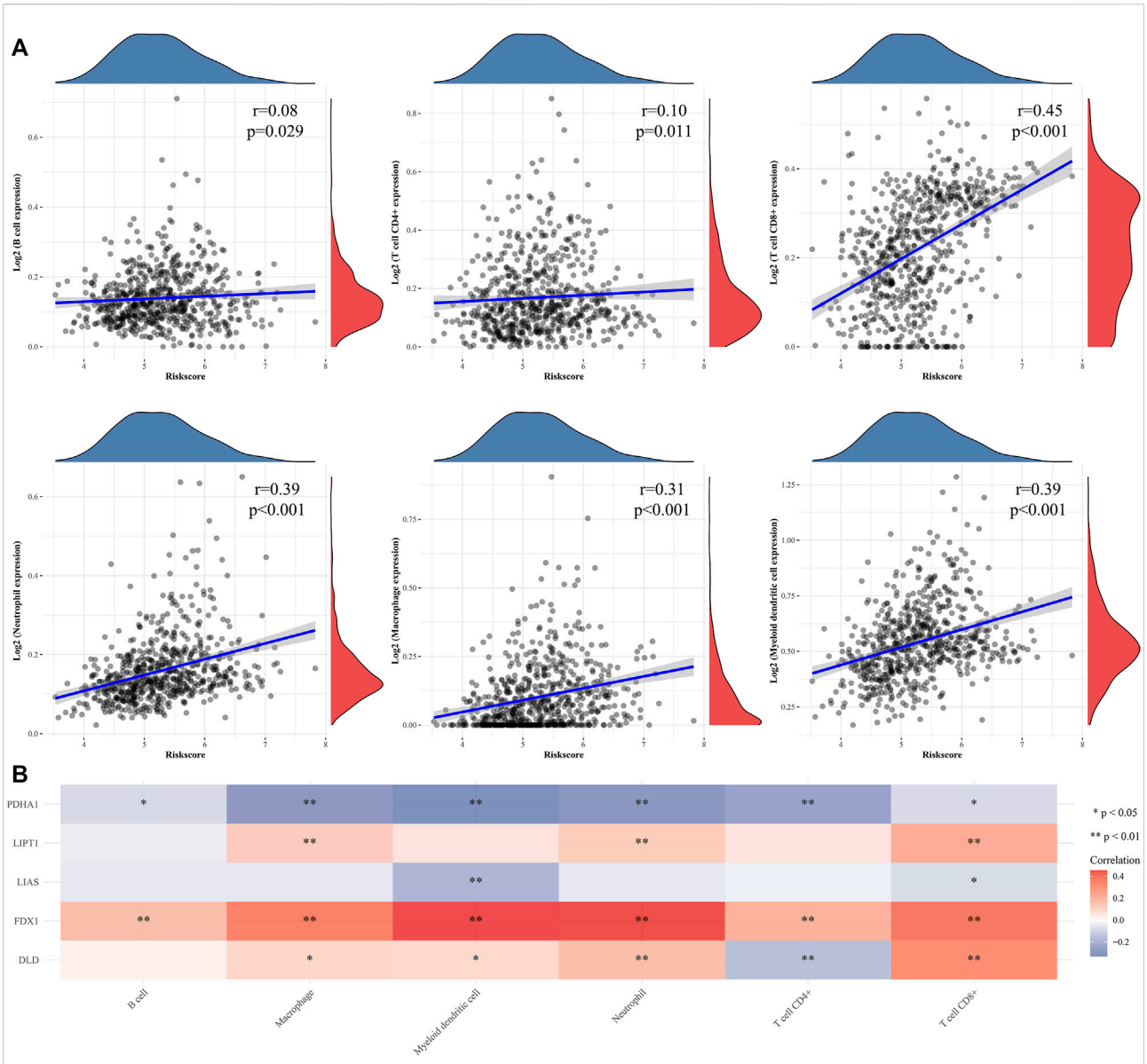

FIGURE 6
Immune infiltration analyse of CRGs signature in gliomas patients. **(A)** The correlations between CRGs signature risk score and immune cell was analysed with Spearman. **(B)** A heatmap of the correlation between CRGs signature genes and immune score. *$p < 0.05$, **$p < 0.01$, ***$p < 0.001$.

3.4 Functional enrichment and immune cell infiltration associated with high and low signature risk scores

We measured the differentially expressed (DE) mRNA levels of gliomas with high and low CRG signature risk scores to explore whether cuproptosis might trigger glioma progression. A volcano plot (Figure 5A) and a heat-map (Figure 5B) identified 1213 DE mRNAs, the expression of 767 of which were increased and 446 decreased (Supplementary Table S3). We sought gene enrichments in terms of biological processes (BP), cellular components (CC), molecular function (MF), and of the criteria of the KEGG (Supplementary Table S4). Neutrophil activation, extracellular structure organization, neutrophil mediated immunity, neutrophil activation involved in immune response, neutrophil degranulation and extracellular matrix organization were all significantly activated on GO-BP enrichment analysis. Phagosome, cell adhesion molecules, *staphylococcus aureus* infection, complement and coagulation cascades and leishmaniasis were enriched on KEGG. The results are shown in Figure 5C. Enrichment results drawn by Metascape were similar (Figure 5D). Immune cell infiltration analysis revealed that the CRG signatures

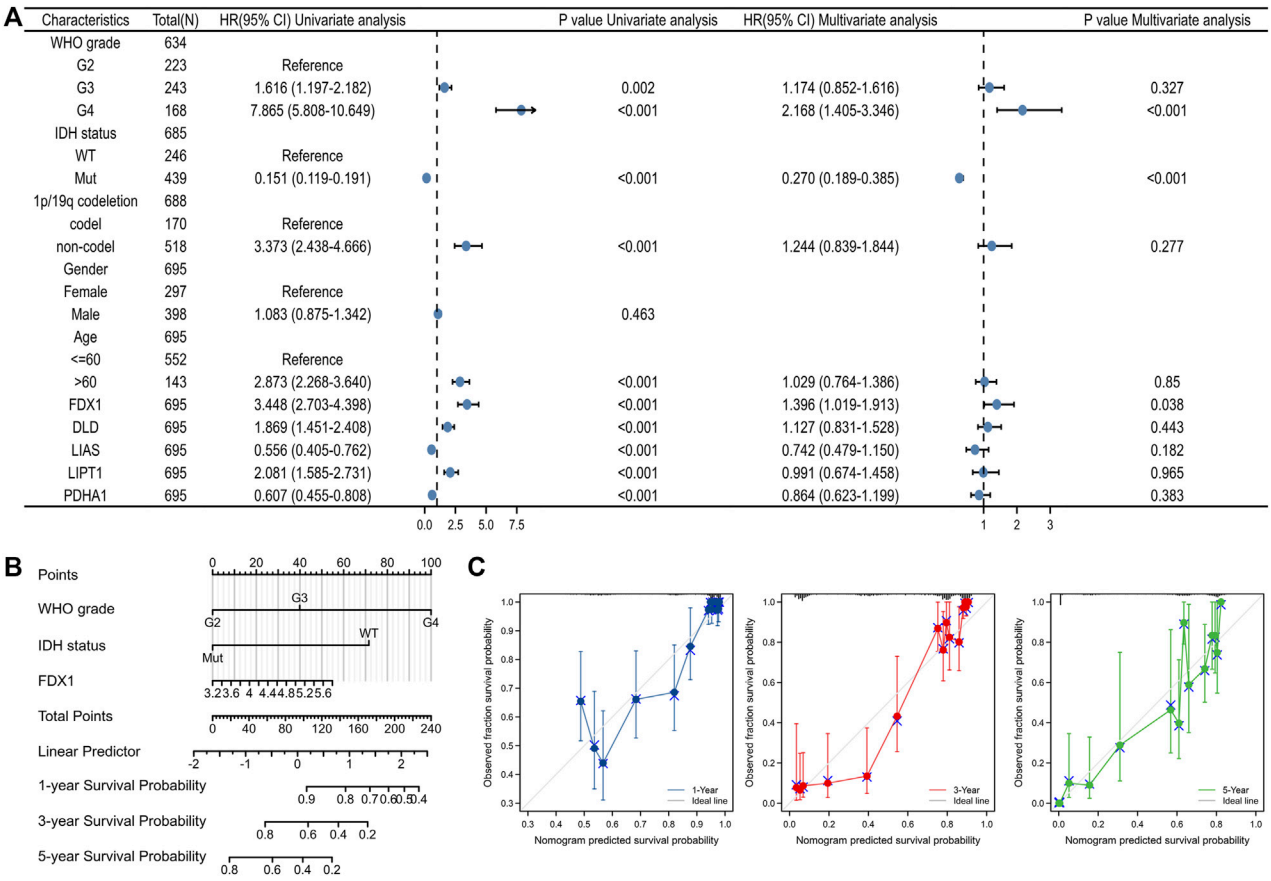

FIGURE 7
Construction of a predictive nomogram. **(A)** The univariate and multivariate Cox regression analysis for clinical parameters of gliomas and five CRGs. **(B)** Nomogram to predict the 1, 3, and 5 years overall survival rate of gliomas patients. **(C)** The calibration curve of the nomogram.

were associated with all six immune cell types, but principally $CD8^+$ T cells (Figure 6A). Figure 6B shows the correlations between the expression levels of CRG signature genes and immune cell activities.

3.5 The nomogram development and construction for gliomas patients

Univariate Cox's regression revealed that a high WHO grade; wild-type IDH status; 1p19q non-co-deletion; age >60 years; high-level expression of FDX1, DLD, and LIPT1; and low-level expression of LIAS and PDHA1 were all associated with poor OS. Multivariate Cox's HR analysis revealed that the WHO grade, IDH status, and the FDX1 mRNA expression level independently predicted OS (Figure 7A). We created an OS nomogram to integrate the FDX1 level with other prognostic factors (the WHO and IDH data) (Figure 7B). We drew a calibration curve to evaluate the contribution of the FDX1 level to nomogram performance; the C-index was 0.834 (0.823–0.846) (Figure 7C). The association between the FDX1 level and the clinicopathological parameters of TCGA patients with gliomas are shown in Table 1. Logistic regression analysis of the FDX1 data revealed strong associations with clinical characteristics including the WHO grade [OR = 3.634 (2.579–5.161), $p < 0.001$]; IDH status [OR = 5.945 (4.20–8.509), $p < 0.001$]; 1p/19q co-deletion [OR = 10.231 (6.492–16.801), $p < 0.001$]; and age (OR = 2.016 (1.384–2.961), $p < 0.001$) (Table 2). Thus, increased FDX1 expression was associated with poor prognosis.

3.6 Validation of the effects of FDX1 levels as revealed by the CGGA and HPA databases

Compared to the low-level FDX1 group of the CGGA database, the high-level FDX1 group evidenced poorer OS [HR = 1.47 (1.12–1.80), log-rank $p < 0.001$) (Figure 8A). The FDX1 level was significantly correlated with the WHO grade ($p < 0.001$) (Figure 8B), IDH status ($p < 0.01$) (Figure 8C), and 1p19q co-deletion status ($p < 0.001$) (Figure 8D). Immunohistochemically, FDX1 staining was positive in gliomas but negative in normal tissues (Figure 8E).

TABLE 1 Association of FDX1 expression and clinicopathological parameters in patients with gliomas.

Characteristic	Low expression of FDX1	High expression of FDX1	*p*
n	348	348	
WHO grade, *n* (%)			<0.001
G2	155 (24.4%)	69 (10.9%)	
G3	130 (20.5%)	113 (17.8%)	
G4	27 (4.3%)	141 (22.2%)	
IDH status, *n* (%)			<0.001
WT	59 (8.6%)	187 (27.3%)	
Mut	287 (41.8%)	153 (22.3%)	
1p/19q codeletion, *n* (%)			<0.001
Codel	148 (21.5%)	23 (3.3%)	
non-codel	200 (29%)	318 (46.2%)	
Gender, *n* (%)			0.818
Female	147 (21.1%)	151 (21.7%)	
Male	201 (28.9%)	197 (28.3%)	
Age, *n* (%)			<0.001
≤60	296 (42.5%)	257 (36.9%)	
>60	52 (7.5%)	91 (13.1%)	
OS event, *n* (%)			<0.001
Alive	262 (37.6%)	162 (23.3%)	
Dead	86 (12.4%)	186 (26.7%)	
DSS event, *n* (%)			<0.001
Alive	266 (39.4%)	165 (24.4%)	
Dead	74 (11%)	170 (25.2%)	
PFI event, *n* (%)			<0.001
Alive	224 (32.2%)	126 (18.1%)	
Dead	124 (17.8%)	222 (31.9%)	
Age, median (IQR)	42 (33, 54)	50 (36, 62)	<0.001

TABLE 2 Logistic regression analysis of FDX1 expression.

Characteristics	Total (N)	Odds ratio (OR)	*p*-Value
WHO grade (G3&G4 vs. G2)	635	3.634 (2.579–5.161)	<0.001
IDH status (WT vs. Mut)	686	5.945 (4.20.-8.509)	<0.001
1p/19q codeletion (non-codel vs. codel)	689	10.231 (6.492–16.801)	<0.001
Age (>60 vs. ≤ 60)	696	2.016 (1.384–2.961)	<0.001
Gender (Male vs. Female)	696	0.954 (0.706–1.288)	0.759

3.7 Correlation between FDX1 expression levels and immune cell infiltration

The correlations between FDX1 expression levels and the numbers of immune cells of 24 different types were assessed. Figure 9A shows the results. The numbers of macrophages, eosinophils, and Th2 cells were significantly positively correlated with the FDX1 expression levels whereas the numbers of pDCs, NK CD56 bright cells, and Treg cells were significantly negatively correlated (Figure 9).

4 Discussion

Gliomas are the most common malignant tumors of the central nervous system, progress rapidly, and are associated

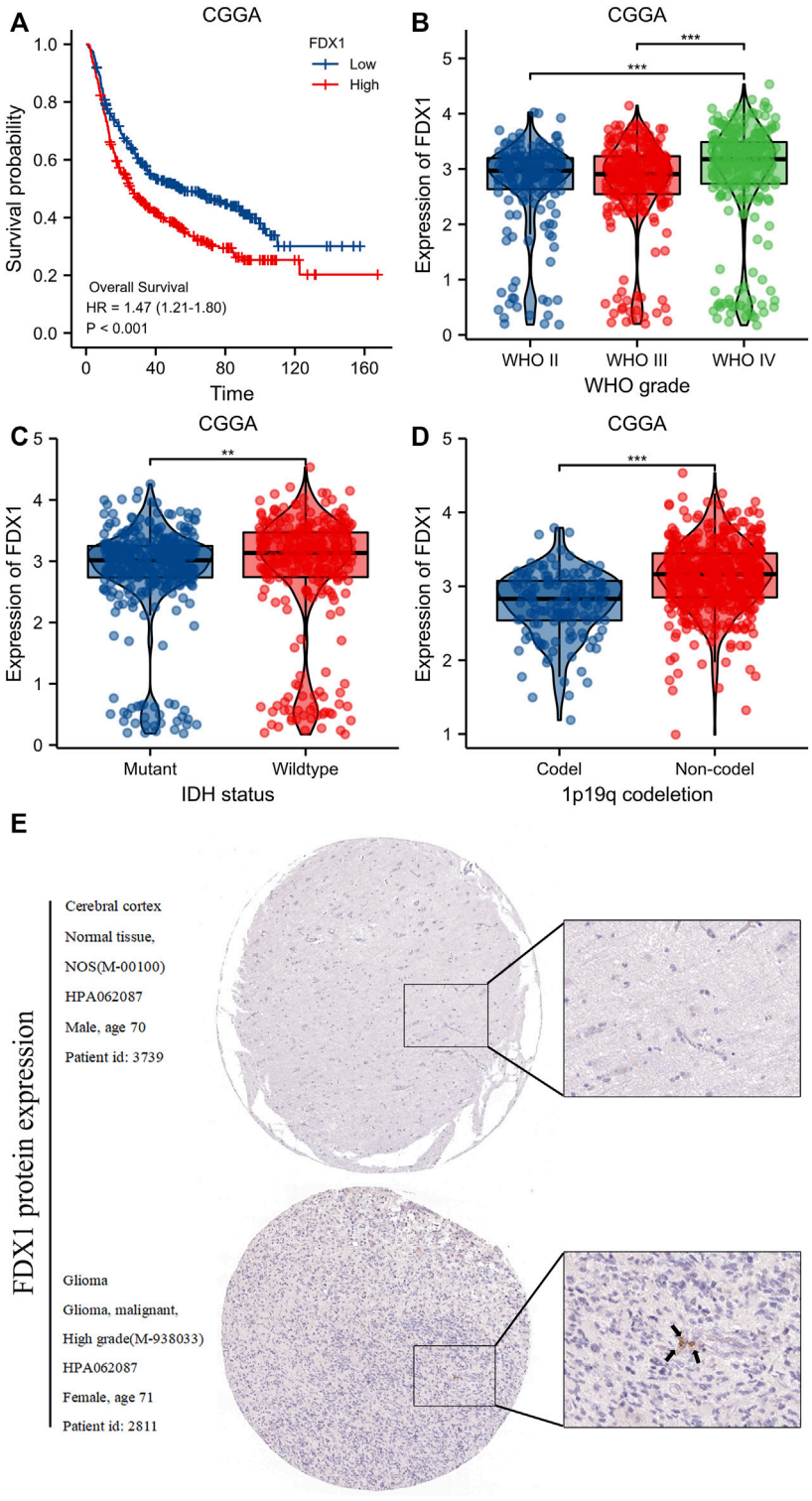

FIGURE 8
Validation of FDX1 expression from CGGA and HPA database. **(A)**Kaplan-Meier survival curve analysis of overall survival (OS) showed that high FDX1 expression correlated to poor prognosis of gliomas patients from CGGA database. **(B–D)** The association of FDX1 expression with WHO grade **(B)**, IDH status **(C)** and 1p/19q codeletion **(D)** in gliomas from CGGA database. **(E)** FDX1 protein expression in gliomas tissues determined using HPA. ***$p < 0.001$, ns, no statistical difference.

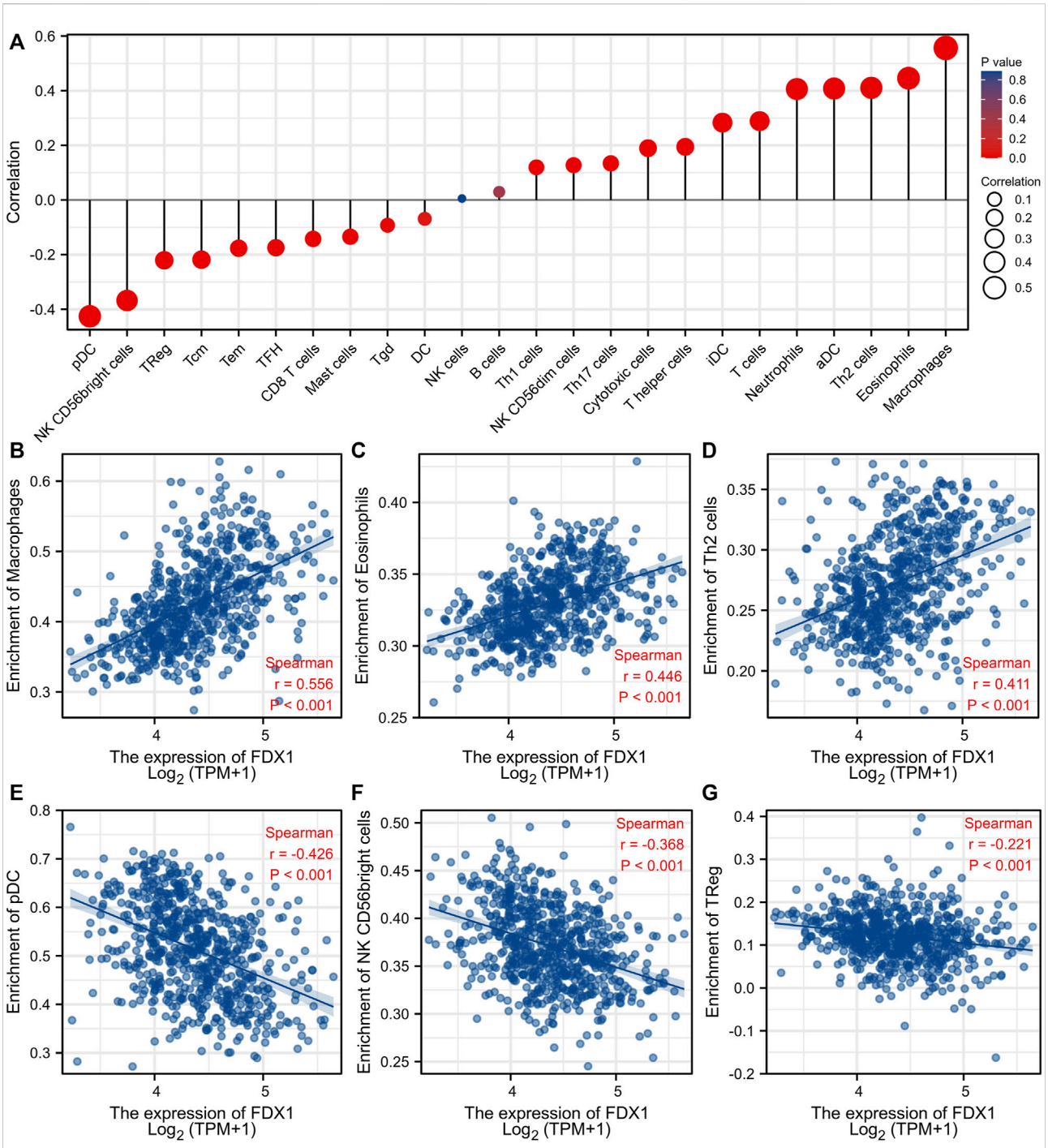

FIGURE 9
Association analysis of FDX1 expression and immune infiltration in gliomas patients. **(A)** The association between FDX1 expression and 24 tumor-infiltrating lymphocytes. **(B–D)** The positive correlation of FDX1 expression with immune infiltration level of Macrophages **(B)**, Eosinophils **(C)**, and Th2 cells**(D)**. **(E–G)** The negative correlation of FDX1 expression with immune infiltration level of pDC cells **(E)**, NK CD56 bright cells **(F)**, and TReg **(G)**.

with poor prognoses and high mortality, imposing significant costs on families and society (Lah et al., 2020; Guo et al., 2021). Early diagnosis, and timely and effective treatment, are critical. Improvements are essential (Muller et al., 2020). Copper binds to the acylated fatty acids of the TCA cycle, triggering toxic protein stress; this is cuproptosis (Tsvetkov

et al., 2022). However, any role for cuproptosis in glioma progression remains poorly understood. We explored the glioma expression levels of 10 CRGs and their prognostic significances. We present a novel, cuproptosis-based, prognostic scoring system. We found that FDX1 might be a valuable therapeutic target.

The expression levels of all 10 CRGs differed between glioma and normal tissues. In addition to the levels of GLS, MTF1, and PDHB, those of the other seven CRGs significantly affected the OS, DSS, and PFI of glioma patients; cuproptosis may play a major role in disease progression. The signature risk scores showed that cuproptosis was highly correlated with tumor immune cell infiltration; cuproptosis may modulate such infiltration.

The "cuproptosis" concept is rather new; few studies on the effects of cuproptosis genes on glioma development have been published. Wang et al. (2022b) subjected CRG data to cluster analysis, and studied the possible roles of genomic mutations and immune cell infiltration in great depth; that study was very valuable. Chen et al. (2022) found that CRG levels were highly correlated with glioma aggressiveness and immune infiltration, and screened potential therapeutic agents, opening a new path toward glioma treatment. Ye et al. (2022) developed a valuable copper death prognostic model for WHO grade 2/3 glioma patients; drug-sensitivity was important. Ouyang et al. (2022) presented models based on lncRNA and CRG levels; cuproptosis-associated glutaminase gene expression reflected the prognosis of glioma patients. The prognostic model of Yan et al. (2022) used the levels of cuproptosis-associated lncRNAs to identify appropriate immune checkpoint blockade (ICB) therapies for LGG patients. We employed LASSO Cox's regression analysis when constructing our prognostic model; the risk score was based on the levels of five CRGs (FDX1, DLD, LIAS, LIPT1, and PDHA1). Our model well-predicted the OS of glioma patients, not only those of the TCGA database but also those of the CGGA database. Our model yields risk scores (numbers), facilitating generalization. In addition, we found that FDX1 status was important in terms of glioma progression.

FDX1 encodes an iron-sulfur protein that reduces Cu^{2+} to Cu^{1+} and regulates protein acylation during cuproptosis (Dorsam and Fahrer, 2016; Weger et al., 2018). DLD is a key enzyme of many dehydrogenase and glycine decarboxylase complexes that maintain cellular and mitochondrial homeostasis (Duarte et al., 2021). LIPT1 and LIAS are members of the lipoic acid metabolic pathway that regulates mitochondrial energy metabolism (Tort et al., 2014; Cronan, 2020). PDHA 1 (a key component of the pyruvate dehydrogenase complex) controls pyruvate entry into the TCA cycle (Echeverri et al., 2021). Univariate Cox's regression confirmed that the FDX1, DLD, LIAS, LIPT1, and PDHA1 levels were all associated with OS, but only the FDX1 level independently predicted survival.

The soluble iron-sulfur protein ferredoxin 1 (FDX1) plays major roles in many metabolic pathways, for example, by transferring electrons during mitochondrial redox reactions (Sawyer and Winkler, 2017). Wang et al. (2021) found that FDX1 was involved in mitochondrial steroid metabolism, and played a role in the development of polycystic ovary syndrome. FDX1 facilitates copper-dependent cell death; an analysis of FDX1 action shed light on how cells respond to proteotoxic stress (Tsvetkov et al., 2019). FDX1 increases ATP production and plays key roles in glucose metabolism, fatty acid oxidation, and amino acid metabolism in lung adenocarcinoma cells (Zhang et al., 2021).

Any prognostic utility of glioma FDX1 status remains unclear. We found that FDX1 status is strongly correlated with glioma prognosis, the WHO glioma grade, IDH status, and 1p19q co-deletion status. The FDX1 level independently predicted glioma prognosis. Immune cells play important roles in tumor creation and development (Chasov et al., 2020). We explored the connections between FDX1 levels and immune cell populations. Higher FDX1 expression strongly enhanced tumor infiltration of macrophages, eosinophils, and Th2 cells but reduced infiltration of pDCs, NK CD56 bright cells, and Treg cells. Thus, FDX1 may regulate immune infiltration into the glioma microenvironment.

Our work had several limitations. Most data were mined from public databases and validated only *in vitro*; some of our findings require further validation. We interrogated only a few databases. Prospective studies with larger sample sizes are needed.

5 Conclusion

We explored the roles played by CRGs in glioma development. Our prognostic risk score based on the expression signature is strongly predictive of OS. The FDX1 level was independently prognostic; targeting of FDX1 expression might serve as a cuproptosis-specific therapeutic strategy for glioma prevention and treatment.

Data availability statement

The original contributions presented in the study are included in the article/Supplementary Material, further inquiries can be directed to the corresponding authors.

Author contributions

Conceptualization, HZ and HO; methodology, HZ and JT; software, QW; validation, HO, XP, and HZ; formal analysis, XP; investigation, HZ; resources, QW; data curation, HZ; writing–original draft preparation, HZ; writing–review and editing, ML; visualization, JT and QW; supervision, YZ; project administration, ML; funding acquisition, YZ and ML. All authors have read and agreed to the published version of the manuscript.

Funding

This research was funded by the natural science foundation of Jiangxi Province (No. 20212BAB206029), the National Natural Science Foundation of China (NSFC) (No. 81860225, 82260248), the key research and development plan of Jiangxi Province (No. 20203BBG73060), and young talents research and cultivation fundation of the First Affiliated Hospital of Nanchang University (No. YFYPY202038).

Conflict of interest

The authors declare that the research was conducted in the absence of any commercial or financial relationships that could be construed as a potential conflict of interest.

Publisher's note

All claims expressed in this article are solely those of the authors and do not necessarily represent those of their affiliated organizations, or those of the publisher, the editors and the reviewers. Any product that may be evaluated in this article, or claim that may be made by its manufacturer, is not guaranteed or endorsed by the publisher.

Supplementary material

The Supplementary Material for this article can be found online at: https://www.frontiersin.org/articles/10.3389/fgene.2022.992995/full#supplementary-material

References

Babak, M. V., and Ahn, D. (2021). Modulation of intracellular copper levels as the mechanism of action of anticancer copper complexes: Clinical relevance. *Biomedicines* 9, 852. doi:10.3390/biomedicines9080852

Blockhuys, S., Celauro, E., Hildesjo, C., Feizi, A., Stal, O., Fierro-Gonzalez, J. C., et al. (2017). Defining the human copper proteome and analysis of its expression variation in cancers. *Metallomics* 9, 112–123. doi:10.1039/c6mt00202a

Brito, C., Azevedo, A., Esteves, S., Marques, A. R., Martins, C., Costa, I., et al. (2019). Clinical insights gained by refining the 2016 who classification of diffuse gliomas with: Egfr amplification, tert mutations, pten deletion and mgmt methylation. *Bmc Cancer* 19, 968. doi:10.1186/s12885-019-6177-0

Chasov, V., Mirgayazova, R., Zmievskaya, E., Khadiullina, R., Valiullina, A., Stephenson, C. J., et al. (2020). Key players in the mutant p53 team: Small molecules, gene editing, immunotherapy. *Front. Oncol.* 10, 1460. doi:10.3389/fonc.2020.01460

Chen, B., Zhou, X., Yang, L., Zhou, H., Meng, M., Zhang, L., et al. (2022). A cuproptosis activation scoring model predicts neoplasm-immunity interactions and personalized treatments in glioma. *Comput. Biol. Med.* 148, 105924. doi:10.1016/j.compbiomed.2022.105924

Chen, R., Smith-Cohn, M., Cohen, A. L., and Colman, H. (2017). Glioma subclassifications and their clinical significance. *Neurotherapeutics* 14, 284–297. doi:10.1007/s13311-017-0519-x

Cronan, J. E. (2020). Progress in the enzymology of the mitochondrial diseases of lipoic acid requiring enzymes. *Front. Genet.* 11, 510. doi:10.3389/fgene.2020.00510

Dixon, S. J., Lemberg, K. M., Lamprecht, M. R., Skouta, R., Zaitsev, E. M., Gleason, C. E., et al. (2012). Ferroptosis: An iron-dependent form of nonapoptotic cell death. *Cell* 149, 1060–1072. doi:10.1016/j.cell.2012.03.042

Dorsam, B., and Fahrer, J. (2016). The disulfide compound alpha-lipoic acid and its derivatives: A novel class of anticancer agents targeting mitochondria. *Cancer Lett.* 371, 12–19. doi:10.1016/j.canlet.2015.11.019

Duarte, I. F., Caio, J., Moedas, M. F., Rodrigues, L. A., Leandro, A. P., Rivera, I. A., et al. (2021). Dihydrolipoamide dehydrogenase, pyruvate oxidation, and acetylation-dependent mechanisms intersecting drug iatrogenesis. *Cell. Mol. Life Sci.* 78, 7451–7468. doi:10.1007/s00018-021-03996-3

Echeverri, R. N., Mohan, V., Wu, J., Scott, S., Kreamer, M., Benej, M., et al. (2021). Dynamic regulation of mitochondrial pyruvate metabolism is necessary for orthotopic pancreatic tumor growth. *Cancer Metab.* 9, 39. doi:10.1186/s40170-021-00275-4

Ge, E. J., Bush, A. I., Casini, A., Cobine, P. A., Cross, J. R., DeNicola, G. M., et al. (2022). Connecting copper and cancer: From transition metal signalling to metalloplasia. *Nat. Rev. Cancer* 22, 102–113. doi:10.1038/s41568-021-00417-2

Gilbert, M. R., Dignam, J. J., Armstrong, T. S., Wefel, J. S., Blumenthal, D. T., Vogelbaum, M. A., et al. (2014). A randomized trial of bevacizumab for newly diagnosed glioblastoma. *N. Engl. J. Med.* 370, 699–708. doi:10.1056/NEJMoa1308573

Gramatzki, D., Dehler, S., Rushing, E. J., Zaugg, K., Hofer, S., Yonekawa, Y., et al. (2016). Glioblastoma in the canton of zurich, Switzerland revisited: 2005 to 2009. *Cancer* 122, 2206–2215. doi:10.1002/cncr.30023

Guo, X., Wang, T., Huang, G., Li, R., Da, C. C., Li, H., et al. (2021). Rediscovering potential molecular targets for glioma therapy through the analysis of the cell of origin, microenvironment and metabolism. *Curr. Cancer Drug Targets* 21, 558–574. doi:10.2174/1568009621666210504091722

Hatori, Y., Yan, Y., Schmidt, K., Furukawa, E., Hasan, N. M., Yang, N., et al. (2016). Neuronal differentiation is associated with a redox-regulated increase of copper flow to the secretory pathway. *Nat. Commun.* 7, 10640. doi:10.1038/ncomms10640

Ishida, S., Andreux, P., Poitry-Yamate, C., Auwerx, J., and Hanahan, D. (2013). Bioavailable copper modulates oxidative phosphorylation and growth of tumors. *Proc. Natl. Acad. Sci. U. S. A.* 110, 19507–19512. doi:10.1073/pnas.1318431110

Lah, T. T., Novak, M., and Breznik, B. (2020). Brain malignancies: Glioblastoma and brain metastases. *Semin. Cancer Biol.* 60, 262–273. doi:10.1016/j.semcancer.2019.10.010

Liang, C., Zhang, X., Yang, M., and Dong, X. (2019). Recent progress in ferroptosis inducers for cancer therapy. *Adv. Mat.* 31, e1904197. doi:10.1002/adma.201904197

Muller, B. J., Kulasinghe, A., Chua, B., Day, B. W., and Punyadeera, C. (2020). Circulating biomarkers in patients with glioblastoma. *Br. J. Cancer* 122, 295–305. doi:10.1038/s41416-019-0603-6

Ouyang, Z., Zhang, H., Lin, W., Su, J., and Wang, X. (2022). Bioinformatic profiling identifies the glutaminase to be a potential novel cuproptosis-related biomarker for glioma. *Front. Cell Dev. Biol.* 10, 982439. doi:10.3389/fcell.2022.982439

Quinones, A., and Le, A. (2018). The multifaceted metabolism of glioblastoma. *Adv. Exp. Med. Biol.* 1063, 59–72. doi:10.1007/978-3-319-77736-8_4

Reifenberger, G., Wirsching, H. G., Knobbe-Thomsen, C. B., and Weller, M. (2017). Advances in the molecular genetics of gliomas - implications for classification and therapy. *Nat. Rev. Clin. Oncol.* 14, 434–452. doi:10.1038/nrclinonc.2016.204

Rouse, C., Gittleman, H., Ostrom, Q. T., Kruchko, C., and Barnholtz-Sloan, J. S. (2010). Years of potential life lost for brain and cns tumors relative to other cancers in adults in the United States. *Neuro. Oncol.* 18, 70–77. doi:10.1093/neuonc/nov249

Sawyer, A., and Winkler, M. (2017). Evolution of chlamydomonas reinhardtii ferredoxins and their interactions with [fefe]-hydrogenases. *Photosynth. Res.* 134, 307–316. doi:10.1007/s11120-017-0409-4

Tort, F., Ferrer-Cortes, X., Thio, M., Navarro-Sastre, A., Matalonga, L., Quintana, E., et al. (2014). Mutations in the lipoyltransferase lipt1 gene cause a fatal disease associated with a specific lipoylation defect of the 2-ketoacid dehydrogenase complexes. *Hum. Mol. Genet.* 23, 1907–1915. doi:10.1093/hmg/ddt585

Tsvetkov, P., Coy, S., Petrova, B., Dreishpoon, M., Verma, A., Abdusamad, M., et al. (2022). Copper induces cell death by targeting lipoylated tca cycle proteins. *Science* 375, 1254–1261. doi:10.1126/science.abf0529

Tsvetkov, P., Detappe, A., Cai, K., Keys, H. R., Brune, Z., Ying, W., et al. (2019). Author correction: Mitochondrial metabolism promotes adaptation to proteotoxic stress. *Nat. Chem. Biol.* 15, 757. doi:10.1038/s41589-019-0315-5

Wang, W., Lu, Z., Wang, M., Liu, Z., Wu, B., Yang, C., et al. (2022). The cuproptosis-related signature associated with the tumor environment and prognosis of patients with glioma. *Front. Immunol.* 13, 998236. doi:10.3389/fimmu.2022.998236

Wang, Y., Zhang, L., and Zhou, F. (2022). Cuproptosis: A new form of programmed cell death. *Cell. Mol. Immunol.* 19, 867–868. doi:10.1038/s41423-022-00866-1

Wang, Z., Dong, H., Yang, L., Yi, P., Wang, Q., and Huang, D. (2021). The role of fdx1 in granulosa cell of polycystic ovary syndrome (pcos). *BMC Endocr. Disord.* 21, 119. doi:10.1186/s12902-021-00775-w

Weger, M., Weger, B. D., Gorling, B., Poschet, G., Yildiz, M., Hell, R., et al. (2018). Glucocorticoid deficiency causes transcriptional and post-transcriptional reprogramming of glutamine metabolism. *Ebiomedicine* 36, 376–389. doi:10.1016/j.ebiom.2018.09.024

Yan, X., Wang, N., Dong, J., Wang, F., Zhang, J., Hu, X., et al. (2022). A cuproptosis-related lncrnas signature for prognosis, chemotherapy, and immune checkpoint blockade therapy of low-grade glioma. *Front. Mol. Biosci.* 9, 966843. doi:10.3389/fmolb.2022.966843

Ye, Z., Zhang, S., Cai, J., Ye, L., Gao, L., Wang, Y., et al. (2022). Development and validation of cuproptosis-associated prognostic signatures in who 2/3 glioma. *Front. Oncol.* 12, 967159. doi:10.3389/fonc.2022.967159

Zhang, Z., Ma, Y., Guo, X., Du, Y., Zhu, Q., Wang, X., et al. (2021). Fdx1 can impact the prognosis and mediate the metabolism of lung adenocarcinoma. *Front. Pharmacol.* 12, 749134. doi:10.3389/fphar.2021.749134